Available online at www.sciencedirect.com

ScienceDirect

journal homepage: www.elsevier.com/locate/he

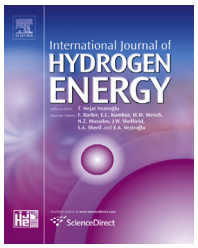

Electronic effect in intermetallic electrocatalysts with low susceptibility to CO poisoning during hydrogen oxidation

F. Bortoloti [a], A.C. Garcia [b], A.C.D. Angelo [a,*]

[a] Electrocatalysis Lab, Chemistry Dept., UNESP, Bauru, SP, Brazil
[b] IQSC, USP, Sao Carlos, SP, Brazil

ARTICLE INFO

Article history:
Received 12 February 2015
Received in revised form
26 June 2015
Accepted 27 June 2015
Available online 26 July 2015

Keywords:
Hydrogen oxidation reaction
CO poisoning
Ordered intermetallic catalysts
PtSn
Electronic effect

ABSTRACT

This paper reports the results of Hydrogen Oxidation Reaction (HOR) experiments over ordered intermetallic (PtSn and PdSn) nanoparticles under CO-free and CO-covered surface conditions. The activity of PtSn toward the HOR was comparable to the activity of commercially available Pt/C. In addition, PtSn/C presented low susceptibility to CO poisoning. In the case of CO-covered surfaces, it was found that the CO was weakly adsorbed at the surface of the PtSn nanoparticles and it did not inhibit the HOR; in fact, this catalyst performed better than Pt/C under the same experimental conditions. X-Ray Absorption assays conducted in the present work proved that the ability of Sn to donate electrons to the Pt adsorption sites was crucial for the resulting intermetallic catalyst to display high activity in the HOR and low susceptibility to CO poisoning.

Introduction

One of the greatest challenges that scientists have to face to implement the use of hydrogen-fed proton-exchange membrane (PEM) fuel cells is to find a way to employ hydrogen fuel obtained from renewable biomass catalytic reform processes effectively. When it comes to producing electricity, hydrogen-fed PEM fuel cells constitute the most efficient electrochemical devices; however, if the fuel contains traces of CO (co-produced during the catalytic reforming process), this contaminant will rapidly poison the catalyst surface and reduce the device power to useless levels. Such passivation process is particularly important at the surface of Pt, the best electrocatalyst for hydrogen oxidation.

One widely applied strategy to overcome the limitation of Pt surface passivation has been to add oxophilic metals to the Pt structure. These metals act in two different ways: (1) they produce oxygenated species at less positive potentials and therefore aid CO removal via the Langmuir–Hinshelwood mechanism, and/or (2) they modify the electronic state of the Pt adsorption sites, which will influence CO adsorption. Both phenomena may contribute to the successful application of fuel cells fed with hydrogen produced from biomass catalytic reform processes. Hence, it is essential to know which of these mechanisms, if not both, underlies the development of CO-poisoning resistance in electrocatalysts. Unfortunately, this type of chemistry does not have a probing species. The electronic effect of the oxophilic metal takes place as soon as the foreign atom is introduced into the structure of the catalyst.

* *Corresponding author.*
E-mail address: acangelo@fc.unesp.br (A.C.D. Angelo).
http://dx.doi.org/10.1016/j.ijhydene.2015.06.145

Then, the bifunctional action may or may not occur. For this reason, it is hard to distinguish the effect through which the oxophilic metal acts in the catalyst, and it is difficult to provide a reliable explanation for the actual role of the foreign metal.

Tin is an oxophilic transition metal with frequent application in noble metal matrixes—Sn enhances the catalytic activity of fuel cell anodes for the oxidation of organic fuels. There is no consensus on whether Sn improves electrode activity via the electronic or bifunctional effect. Sn ([Kr] $4d^{10}5s^25p^2$) exerts an electron donor effect toward the Pt orbitals, which increases the electron density of the Pt ([Xe] $4f^{14}5d^96s^1$) adsorption sites. This action is particularly effective in the Pt sites because the half-filled d-orbital of Pt favors this phenomenon. In contrast, the electronic configuration of Pd ([Kr] 4 d^{10}) does not facilitate the donor action of Sn atoms because the Pd d-orbitals are already filled. In parallel, the oxophilic character of Sn atoms will always be present at the surface of noble metals, to generate oxygenated species (−OH, −OOH, $-O_2$) at less positive electrode potentials than in the case of the pure noble metals. On the basis of the aforementioned characteristics, the electronic and the bifunctional effect will predominate at the PtSn and the PdSn surfaces, respectively. In this context, this investigation has relied on the CO oxidation reaction to evaluate the ability of PtSn and PdSn surfaces to adsorb CO, suffer CO poisoning, and remain active for the HOR.

Several authors have reported that the bifunctional mechanism and the electronic effect account for the different electrocatalytic activities of PtSn/C and Pt/C during the methanol and ethanol electrooxidation reactions [1–4]. According to Mukerjee and McBreen [5], Sn acts as an electron donor that partially fills the Pt d band and increases the Pt–Pt bond length, which accounts for the distinct performances of PtSn/C and Pt/C. On the basis of XPS and XANES studies, Shukla et al. [6] have proposed that the different electronegativity of Sn and Pt atoms polarizes the Pt–Sn bond, so the donor effect of Sn will give rise to a distinct activity in PtSn/C. Shukla et al. [6] have provided a very consistent explanation for the electronic and bifunctional role that Sn plays in PtSn materials. These authors stated that CO chemisorption on Pt involves donation of an electron pair from CO anti-ligand orbitals to empty Pt 5d orbitals. Back donation of electrons from Pt to CO orbitals stabilizes the Pt–CO interaction even further. On the other hand, partial electron donation to the Pt adsorption site raises the electronic density on the Pt atom, which decreases the energy of the interaction between CO and the Pt adsorption sites. This phenomenon, combined with OH adsorption at the Sn surface sites, aids surface CO removal for anode oxidation of fuel alcohols [6]. Lee et al. [7] studied the CO tolerance in the hydrogen oxidation reaction on Pt/C, PtSn/C and PtRu/C nanoparticles, in PEM fuel cell. According to their results, the onset potential for each material was different, in the order PtSn/C < PtRu/C < Pt/C. The authors proposed that the process of CO adsorption took place through the hydrogen displacement step for PtSn/C, while for PtRu/C and Pt/C was through direct CO adsorption on the free site. Moreover, they observed that the CO adsorption configuration (bridge or linear) was dependent on the material and temperature of cell operation. It was concluded that the thermodynamic and kinect alterations provoked by the alloys were responsible for the higher tolerance to CO poisoning. Crabb, Marshall and Thompsett [8] prepared PtSn bimetallic catalysts supported on Carbon in different compositions, and they studied the influence of this on the CO electrooxidation reaction. The results obtained pointed to the lowering of the CO electrooxidation onset potential on the synthesized materials as compared to Pt/C. Wang and Hsing [9], by using impedance technique, studied H_2/CO electrooxidation kinects at Pt and its alloys surfaces. The higher PtSn/C activity toward the H_2/CO oxidation was attributed by the authors to the combination of several factors, namely: promotion of the OH nucleation; excluding CO adsorption on Sn sites; and the minimization of the CO adsorption caused by the metallic bond. Arenz and coworkers [10] studied the catalytic activity of three PtSn catalysts supported on Carbon toward the CO and H_2/CO electrooxidation reaction. These catalysts differ because of the relative amounts of Pt_3Sn, PtSn and SnO_2 on the support. It was concluded that the material composed exclusively by Pt_3Sn showed the best performance toward the reaction investigated. However, any deeper conclusion on the influence of the materials properties is hard to be extracted due to the presence of a mixture of phases. García-Rodríguez et al. [11] synthesized nanoparticles by incorporating Sn on Pt/C. With these materials, the authors studied the ethanol and CO electrooxidation reactions. According to the results the performance of the materials was dependent on the amount of the Pt_3Sn phase, i.e. the higher the Pt_3Sn amount, lower the onset potentials and higher the current densities for both reactions. The higher ability to CO oxidation was attributed to the Sn-OH_{ads} formed at less positive potentials in comparison to pure Pt. Lim and co-workers [12] synthesized PtSn/C electrocatalysts and evaluated them as anode for low temperature fuel cell. On commercially available Pt/C material, the CO oxidation reaction onset potential and maximum current density potential were more positives than the obtained with PtSn/C catalysts. The authors stated that the Sn promoted the CO_{ads} oxidation in lower potentials due to the ability to adsorb OH specie. Pt_3Sn showed better performance than Pt/C toward the H_2 and H_2/CO oxidation reactions in fuel cell. Such a behavior was considered as consequence of the presence of PtSn alloys and coexistence of the Sn oxides species. A very interesting work was published by Liu, Jackson and Eichhorn [13] that synthesized PtSn alloy, core-shell and intermetallic nanoparticle materials with same composition and particle size and evaluated as anode for H_2 electrooxidation reaction in the presence of CO. RDE tests showed that intermetallic and core–shell structures presented higher performance than Pt, PtRu alloy and PtSn alloy. The authors attributed these results to the electronic effect provoked by PtSn in the core–shell structure while on intermetallic material it was due to the bifunctional effect. Liu et al. [14] reported the study performed with Pt_3Sn nanoparticles toward the CO and methanol electrooxidation reactions. The improved activity of the material for CO oxidation was proposed because of the Sn effect of weakening CO adsorption on Pt and promoting Sn-OH_{ads} formation that eases the near adsorbed CO oxidation process. Moreover, the authors reported that the particles were also very active toward the methanol oxidation reaction. Herranz and colleagues [15] synthesized Pt_3Sn (fcc) and PtSn (hcp)

intermetallic phases to investigated their performance toward the CO and methanol oxidation reactions. The authors considered the better performance of the Pt_3Sn (fcc) phase in comparison to the PtSn (hcp) phase regarding the current densities generated. However, it was stated that the selectivity for the CO reaction seemed to be better than on PtSn (hcp). More recently, it was published a helpful article where the authors prepared PtSn nanoparticles and studied the chemical oxidation of CO to CO_2 [16]. The activation energy determined for the reaction on Pt/C was 133 kJ/mol while for PtSn/C was four times lower, 35 kJ/mol. According to the authors, Sn atoms offer to the surface a distinct site for O_2 adsorption that, on its turn, will act effectively in the process of CO_2 generation.

Concerning PdSn/C electrodes, studies on how Sn affects Pd are still scarce. Zhang and co-workers [17] have suggested that the addition of Sn to the Pd matrix modifies the electronic structure of Pd and elicits an electronic catalytic effect. Such effect increases as the amount of Sn in the matrix augments. Indeed, XPS measurements have shown that the Pd ($3d_{5/2}$) and Pd ($3d_{3/2}$) binding energies shift to lower values—about 0.5 eV (PdSn, 2:1) and 0.7 eV (PdSn/C, 1:1) as compared with the Pd/C catalyst [17]. The negative shift in the binding energy peaks of Pd (3d) means that the addition of Sn and the partial electron transfer from Sn to Pd lower the binding energy.

Notwithstanding the aforementioned papers on the interpretation of the role of the electron donor atom in Pt adsorption sites, a question remains: How much do the electronic and bifunctional effects inhibit CO poisoning on noble metal surface sites?

This paper describes studies on the HOR and CO adsorption at Pt, PtSn, and PdSn surfaces in alkaline medium. Our aim was to assess the importance of the electronic state of the noble metal site and of the bifunctional effect provided by the oxophilic metal for the HOR and CO adsorption.

Experimental

Ordered intermetallic PtSn or PdSn nanoparticles supported on Carbon (Vulcan XC-72, Cabot) were synthesized via the polyol route proposed by Schaak [18]. To this end, proper amounts of $H_2Cl_6Pt.6H_2O$ (Merck, p.a.) or $PdCl_2$ (Sigma Aldrich, 99%) and $SnCl_2$ (Merck, p.a.) were dissolved in tetraethylene glycol (TEG, Sigma–Aldrich, 99%) in the presence of Carbon (Vulcan XC-72) previously treated in N_2 (White Martins, 3.0) atmosphere at 400 °C for 4 h. Polyvinylpyrrolidone (PVP, Sigma–Aldrich, p.a.) served as dispersing agent and stabilizer. Sodium Borohydride ($NaBH_4$, Sigma–Aldrich, 98%) was employed as an auxiliary reducing agent. Further details of the synthesis are available in our previous paper [19]. The performance of the synthesized material was compared with the performance of commercially available Pt/C (E-TEK). X-Ray diffraction (XRD) revealed that the product consisted of ordered intermetallic PtSn and PdSn. A Powder Method setup was used in the X-Ray Diffractometer Rigaku Ultima IV; a Cu anode operating at 40 kV and 20 mA was the X-Ray source (Cu Kα, $\lambda = 1.5406$ Å). The diffractograms were recorded for 2θ values ranging from 20 to 100, at a scan rate of 1°/min. The material was also examined under a ZEISS LEO 440 Scanning Electron Microscope (SEM) coupled to an Energy Dispersive X-Ray Analyzer (EDX Link Analytical). Co served as calibrator; the operating parameters were as follows: electron beam energy = 20 kV, focal distance = 25 mm, dead time = 30%, current = 2.82 A, and I probe = 950 pA. To estimate the relative amount of metals in the sample, five points were randomly selected on the surface. To enable visualization of individual or agglomerated particles, the sample was observed under a Transmission Electron Microscope (JEOL JEM 2100) operating at 200 kW. The materials were deposited on a polished Glassy Carbon surface as a thin film obtained from a dispersion consisting of the supported nanoparticles, isopropyl alcohol, Nafion® (Nafion 117, Aldrich), and deionized water. The as-prepared surface was employed in the electrochemical studies. For such electrochemical studies (cyclic voltammetry and rotating disc electrode), KOH (Merck, p.a.) was used as a 0.2 mol/L solution at 25 ± 1 °C; a large surface Pt wire and Reversible Hydrogen Electrode (RHE) worked as the counter-electrode and reference electrode, respectively. In cyclic voltammetry experiments were performed 100 cycles to achieve a reproducible voltammetric profile; however, usually an unchanged profile was reached around the 10th cycle.

The Hydrogen Oxidation Reaction (HOR) was studied by employing the Rotating Disc Electrode (RDE) technique (Pine Instruments experimental setup). The electrochemical data of the PtSn/C and PdSn/C materials were collected by means of the Linear Sweep Voltammetry technique as the RDE was operating at several rotating rates (100–3500 rpm) at potentials ranging from 0 to 0.4 V, or if otherwise stated. To evaluate how the electrode materials performed at deliberately CO-poisoned surfaces, CO was deposited on each surface by potentiostatic polarization at 0.15 V in a CO-saturated KOH solution 0.2 mol/L, for 30 s. Next, CO was completely removed from the solution by purging N_2. Then, the same procedure described earlier for the HOR study was applied.

To investigate the electronic properties changes caused by the presence of Sn in the PtSn ordered intermetallic material in situ X-Ray Absorption Spectrometry (XAS) analyses in the X-Ray Absorption Near Edge Structure (XANES) were carried out since XANES and the Extended X-Ray Absorption Fine Structure (EXAFS) regions helped to characterize the materials from an electronic and structure standpoint. Experiments were accomplished at Pt L_3 edge. This corresponded to energy of 11564 eV, where the $2p_{3/2} - 5d$ transition occurs and emerges as a broad absorption peak (white line). The magnitude of this peak is correlated to the 5d electronic state occupation—the more intense the peak, the higher the 5d state vacancy. The XAS measurements conducted in this work allowed for evaluation of the valence band vacancy in the PtSn ordered intermetallic material polarized at 0.5 and 0.6 V. All XAS experiments were carried out at the D04B-XAFS1 beam line in the National Synchrotron Light Source Laboratory (LNLS), situated in Campinas, Brazil. X-ray absorption spectra were collected in transmission mode with three ionization chambers (incidence I_0, transmitted I_t, and reference I_r). The reference channel was used mainly to calibrate the edge position with a pure Pt foil sample. The working electrodes employed for the measurements consisted of appropriated amount of catalysts (Pt metal load of 6 mg cm^{-2}) bound with Nafion (5 wt.%) suspended in isopropyl alcohol and carried to

ultrasonic homogenization, after the solvent was evaporated at room temperature. The catalyst powder was then deposited on a disc of carbon cloth (geometric area = 0.95 cm^2) and pressed at room temperature.

Results and discussion

Characterization

Fig. 1 presents the XRD profiles of the materials PtSn/C and PdSn/C. Comparison with data available in Crysmet Files [20] aided unequivocal identification of the materials as ordered intermetallic PtSn and PdSn anchored on Carbon. In addition, PtSn and PdSn belonged to the hexagonal and orthorhombic crystalline systems, respectively. The XRD patterns did not reveal any impurities. XRD data are displayed in Table 1.

Table 2 lists the EDX data of the materials. The experimental compositional results and the nominal composition desired for a 1:1 stoichiometry agreed well.

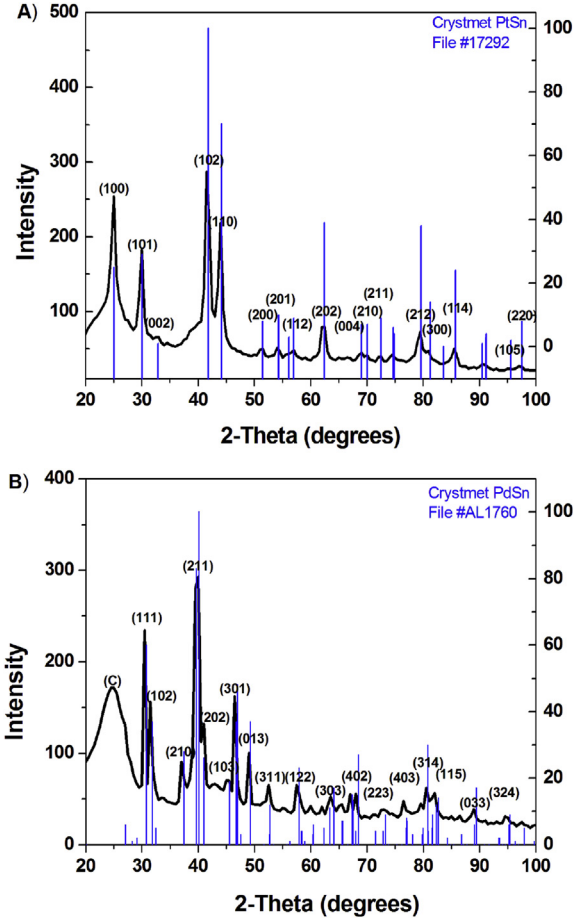

Fig. 1 – X-Ray diffractograms of the ordered intermetallic (A) PtSn/C and (B) PdSn/C nanoparticles at room temperature. The black profile refers to the recorded curve; the blue lines correspond to data for the standard materials compiled in the Database: PtSn (ID: 17292) and PdSn (ID: AL1760).

Fig. 2 displays the TEM images and histograms constructed by using the diameters measured for the metallic particles anchored on the Carbon surface. Although a number of agglomerates emerged, the average particle size was about 1–2 nm for both materials.

Taken together, these results led to the conclusion that the ordered intermetallic PtSn and PdSn nanoparticles anchored on Carbon existed at a stoichiometric ratio of 1:1 and had average diameter of 1–2 nm.

Electrochemical studies

Fig. 3 shows the voltammetric profiles recorded for the synthesized nanoparticles PtSn and PdSn and for the commercially available Pt nanoparticle in KOH solution. The profiles were reproducible even after 100 cycles between 0.05 and 1.2 V. Hence, the nanoparticles were remarkably stable under the experimental electrochemical conditions used in this work. PtSn and Pt displayed similar voltammetric profiles, as discussed in the literature [19]. The capacitive current was higher for Pt because the more dispersed Pt nanoparticles (as mentioned in the characterization section) generated a larger surface area. Despite the similar voltammetric profiles of PtSn and Pt, the electrochemical responses of these materials differed in the presence of the fuel and CO, as discussed later in this work. For PdSn, no peaks arose in the hydrogen region, and the voltammetric profile was poorly defined. It could not be disregarded any aggregation of the particles because of the cycling procedure.

Fig. 4 illustrates the RDE curves of the HOR accomplished on the different electrode surfaces and the corresponding Koutecky-Levich plots. Pt and PtSn exhibited the expected limiting curves, whereas PdSn presented overpotential of about 200 mV. According to analysis of the kinetic results summarized in Table 3, PtSn/C had improved activity as compared with commercial Pt/C under the same experimental conditions. Earlier experimental [21] and theoretical studies [22] had reported enhanced PtSn electrochemical activity toward the HOR. One of these studies [22] explained that electronic contribution from the Sn atoms to the Pt adsorption sites favored H_2 adsorption and facilitated the further steps involved in the HOR. In contrast, PdSn/C was poorly active for the HOR, as evidenced by the thermodynamic (overpotential of 200 mV) and kinetic (kinetic current) parameters. Theoretical calculations performed earlier by our group [22] had predicted this behavior. So far, only the electronic effect could account for the electrochemical performances of the materials reported herein, because none of the adsorbed species would demand a bifunctional action. Moreover, on the basis of the analysis of the electronic configuration of the noble metals mentioned above, it would be reasonable to propose that any donor action by the Sn atom would modify the electronic density of the Pt adsorption sites more efficiently as compared with the Pd adsorption sites. Therefore, this first set of results support the conclusion that the high activity of Pt and PtSn materials toward the HOR originated from the electronic density of the Pt adsorption sites.

The kinetics parameters were calculated from Koutecky–Levich equation:

Table 1 – XRD and mean sizes data obtained for the PtSn/C and PdSn/C nanoparticles.

Material	System	Space group	Lattice parameter (Å)			Crystallite size (DRX) nm	Particle size (TEM) nm
			a	b	c		
PtSn	Hexagonal	$P6_3/mmc$ (194)	4.101	4.101	5.441	7.8	1–2
PdSn	Orthorhombic	Pnma (62)	6.130	3.867	6.320	5.8	1–2

Table 2 – Mean atomic percentages of the elements in the synthesized materials PtSn/C and PdSn/C.

Materials	Mean atomic percentage		
	Pt	Pd	Sn
PtSn/C	48.3 ± 2.5	–	51.7 ± 2.5
PdSn/C	–	50.1 ± 0.5	49.9 ± 0.5

$$\frac{1}{i}=\frac{1}{i_d}+\frac{1}{i_k}=\frac{1}{i_k}+\frac{1}{B\cdot c_0\omega^{-1/2}}$$

where: i_k is the kinetic current density, i_d is the diffusion-limited density, Bc_o is a constant related to the number of electrons transferred in a reaction, the gas concentration and diffusivity, and the electrolyte kinematic viscosity.

To investigate the extent to which a possible bifunctional effect could improve the performance of Pt/C, PtSn/C, and PdSn/C bearing the surface intentionally covered with CO, the RDE curves depicted in Fig. 5 (and the corresponding Koutecky-Levich plots as inserts) were recorded. Complete inhibition of the HOR took place at the CO–PdSn/C surface. The CO–Pt/C surface gave rise to overpotential of 200 mV. The HOR kinetic current decreased to 1/5 and 1/8 of the value

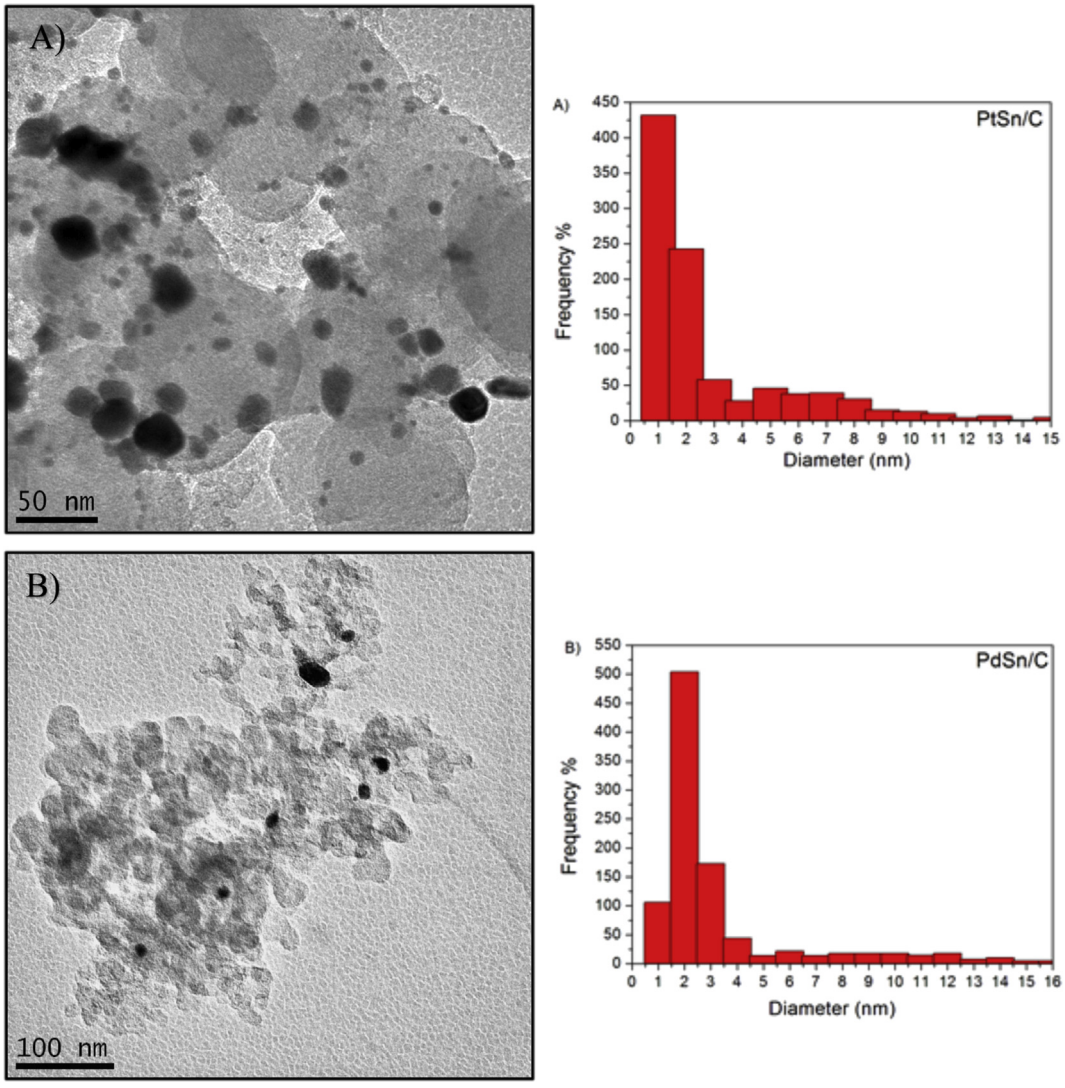

Fig. 2 – TEM images and corresponding histograms for the average particle diameter of ordered intermetallic (A) PtSn and (B) PdSn nanoparticles.

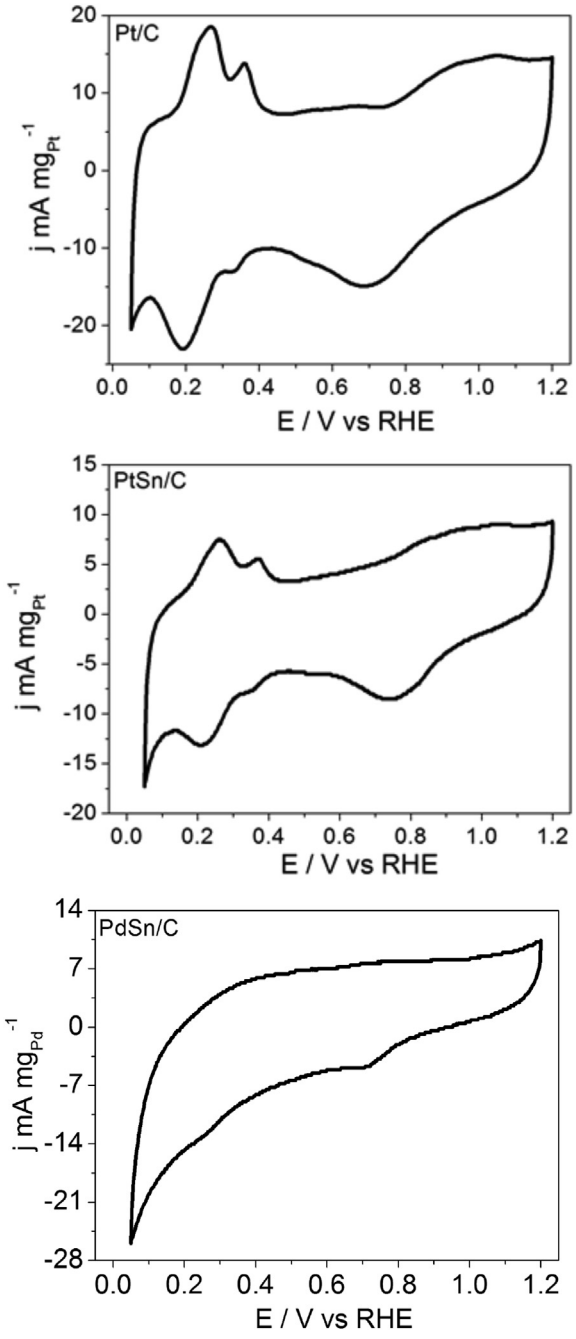

Fig. 3 – Cyclic voltammograms recorded for Pt/C (E-TEK), ordered intermetallic PtSn/C, and ordered intermetallic PdSn/C in KOH 0.2 mol/L, at room temperature.

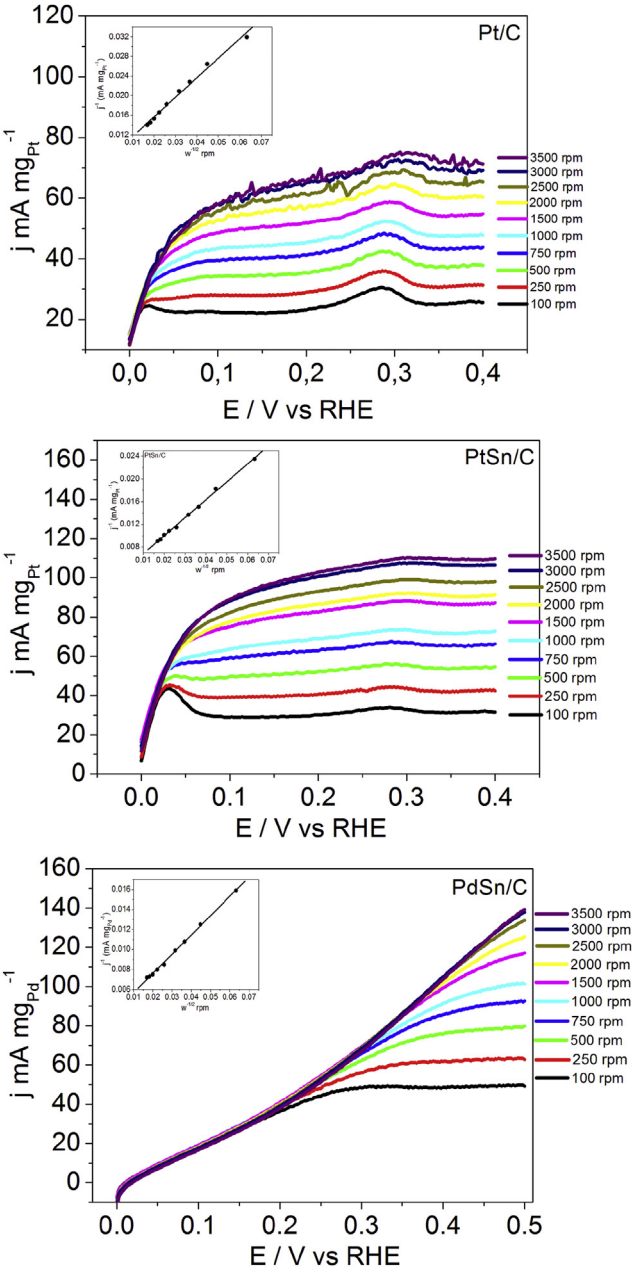

Fig. 4 – RDE curves recorded for the HOR on the Pt/C, PtSn/C, and PdSn/C materials in KOH 0.2 mol/L, at room temperature, for different rotation speeds. The inserts correspond to the Koutecky-Levich plots constructed on the basis of the data collected at 0.4 V to Pt/C, PtSn/C and 0.5 V to PdSn/C.

registered at the corresponding surfaces without CO for the CO–Pt/C and the CO–PdSn/C surfaces, respectively.

Concerning CO–PtSn/C, it yielded a completely distinct and very promising result toward the HOR: (1) the RDE curves split into two waves, showing that the HOR happened at two different surface sites and involved distinct energies; (2) the overpotential was far smaller than the overpotential observed for the CO–Pt/C surface, which suggested lower inhibition of the HOR; and (3) the kinetic current lowered only about 50%. Pinto et al. [23] have published data regarding calculations of CO adsorption at Pt, PtSn, and PdSn surfaces. These authors determined slightly lower adsorption energies (ΔG_{ad}) for CO adsorption at the PdSn surface (−0.46 and −0.57 eV for the on-top and bridge configurations, respectively) as compared with CO adsorption at the PtSn surface (−0.31 and −0.44 eV for the on-top and bridge configurations respectively). This reinforces the experimental result that CO adsorbed spontaneously (in zero charge condition) and more energetically at the PdSn surface as compared with the PtSn surface. Stripping of the CO deposited on each material surface revealed that the charges

Table 3 – Kinetic parameters extracted from the Koutecky-Levich plots constructed for the HOR at different surface conditions, in KOH 0.2 M, at room temperature.

Material	Clean surfaces			CO-deposited surfaces		
	i_k (mA)	i_d max(mA)	$c_o.B$ (mA rpm$^{-1/2}$)	i_k (mA)	i_d max(mA)	$c_o.B$ (mA rpm$^{-1/2}$)
Pt/C	1.30	0.71	2.51×10^{-2}	0.26	0.47	2.36×10^{-2}
PtSn/C	1.61	0.66	1.90×10^{-2}	0.78	0.55	3.11×10^{-2}
PdSn/C	1.26	0.65	2.43×10^{-2}	0.16	0.14	2.55×10^{-2}

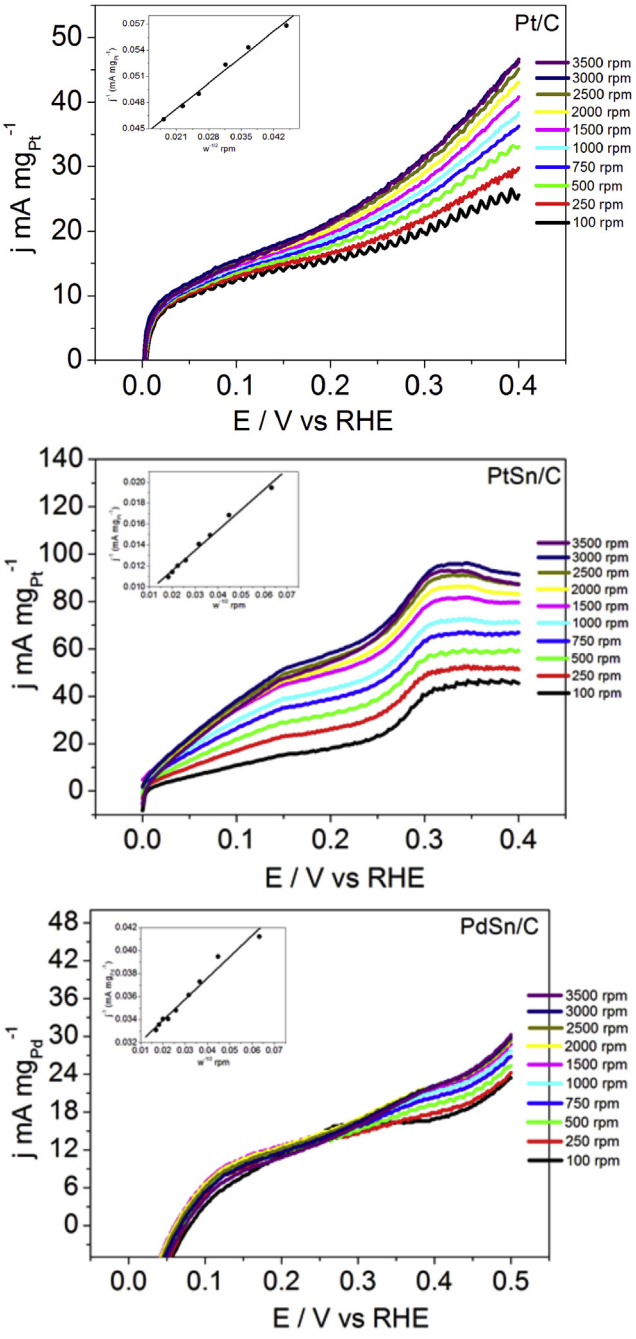

Fig. 5 – RDE curves recorded for the HOR on the CO–Pt/C, CO–PtSn/C and CO–PdSn/C materials in KOH 0.2 mol/L, at room temperature, for different rotation speeds. The inserts correspond to the Koutecky-Levich plots constructed on the basis of the data collected at 0.2 V to Pt/C, PtSn/C and 0.5 V to PdSn/C.

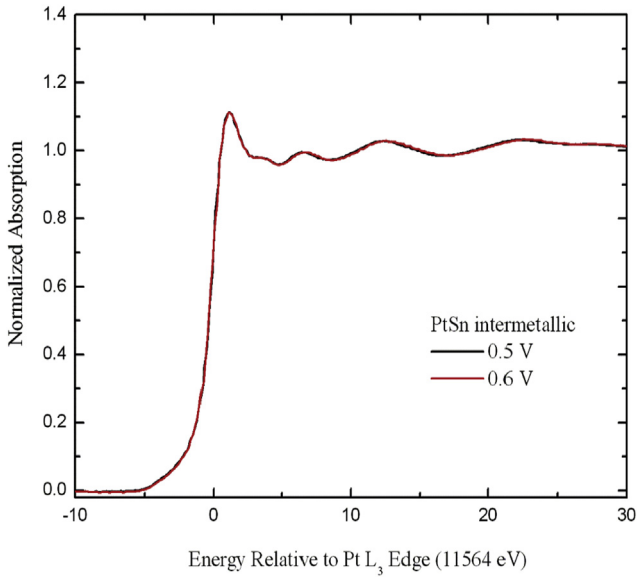

Fig. 6 – Pt L_3 edge XANES spectra of the ordered intermetallic PtSn material. E = 0.5 and 0.6 V vs RHE.

involved in the process were 67, 200, and 4900 μC for the same geometric area and amount of PtSn/C, Pt/C, and PdSn/C materials, respectively. The corresponding onset potentials were 0.38, 0.49, and 0.65 V, respectively. These results pointed out

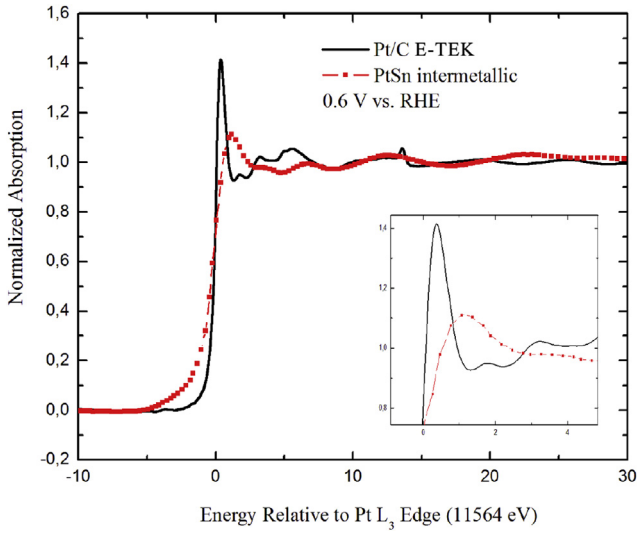

Fig. 7 – Pt L_3 edge XANES spectra of Pt and PtSn. E = 0.6 V vs RHE.

that a lower amount of CO was weakly adsorbed at the PtSn/C surface as compared with the other materials under the same experimental conditions. These results agreed well with data cited earlier in the theoretical study [23]. Indeed, the latter study mentioned that CO seemed to be a much stronger poison for the PdSn surface, whilst the PtSn/C surface was less susceptible to CO poisoning. Thus, the oxophilic element Sn did not seem to affect the CO desorption process via a bifunctional action—both the theoretical and experimental results strongly suggested that the final electronic configuration of the adsorption sites was the factor that culminated in the best performance of the PtSn/C material as compared with Pt/C and PdSn/C.

Fig. 6 contains the Pt L_3 edge XANES spectra recorded for ordered intermetallic PtSn at two different potentials. The two spectra overlapped perfectly, suggesting that the white line was the same. Therefore, the adsorbed OH species produced at 0.6 V did not modify the Pt electronic state.

Fig. 7 compares the Pt L_3 XANES spectra of the ordered intermetallic PtSn material and of the commercially available Pt (E-TEK) at 0.6 V. The white line of the PtSn material became less intense, suggesting that Sn did alter the Pt electronic state. The lower intensity of the white line resulted from the electron donor effect of the Sn atom to Pt. The energy of the PtSn band shifted, corroborating the electron donor effect. This effect diminished the electronic back donation exerted by the CO species, which then weakened the Pt—CO bond and abated the CO poisoning effect at the PtSn surface.

Conclusions

The electronic state of the adsorption sites in nanoparticle materials containing a noble metal element underlay the improved electrochemical activity of the investigated ordered intermetallic materials. The PtSn nanoparticle was a better electrocatalyst for the HOR and less susceptible to CO poisoning than Pt. The ordered intermetallic PdSn nanoparticle performed the least efficiently toward the HOR at clean surfaces. XAS studies suggested that the lower susceptibility to CO poisoning of the ordered intermetallic PtSn material stemmed from decreased electronic retro-donation effect from CO toward Pt. This effect weakened the Pt—CO interaction and led to lower coverage of the Pt surface with CO. Even though theoretical studies are not appropriate to interpret phenomena occurring at nanoparticle materials, the results exposed herein agree very well with data predicted by the DFT computational method.

Acknowledgments

Authors are grateful to Fundação de Amparo à Pesquisa do Estado de São Paulo (FAPESP #2013/05634-8) for the financial support of this work. F. Bortoloti thanks FAPESP for the undergraduate fellowship (#2010/07798-0). The authors also thank to Professor H.M. Villulas for performing XAS measurements and Brazilian National Laboratory of Synchrotron Light (LNLS) for the XAS analyses.

REFERENCES

[1] Colmati F, Antonili E, Gonzalez ER. Pt—Sn/C electrocatalysts for methanol oxidation synthesized by reduction with formic acid. Electrochim Acta 2005;50:5496—503.
[2] Zhou WJ, Song SQ, Li WZ, Zhou ZH, Sun GQ, Xin Q, et al. Direct ethanol fuel cells based on PtSn anodes: the effect of Sn content on the fuel cell performance. J Power Sources 2005;140:50—8.
[3] Vigier F, Coutanceau C, Hahn F, Belgsir EM, Lamy C. On the mechanism of ethanol electro-oxidation on Pt and PtSn catalysts: electrochemical and in situ IR reflectance spectroscopy studies. J Electroanal Chem 2004;563:81—9.
[4] Frelink T, Visscher W, van Veen JAR. On the role of Ru and Sn as promoters of metanol electro-oxidation over Pt. Surf Sci 1995;335:353—60.
[5] Mukerjee S, McBreen J. An in situ X-Ray absorption spectroscopy investigation of the effect of Sn additions to carbon-supported Pt electrocatalysts Part I. J Electrochem Soc 1999;146:600—6.
[6] Shukla AK, Arico AS, El-Khatib KM, Kim H, Antonucci PL, Antonucci V. An X-ray photoelectron spectroscopic study on the effect of Ru and Sn additions to platinised carbons. Appl Surf Sci 1999;137:20—9.
[7] Lee SJ, Mukerjee S, Ticianelli EA, McBreen. Electrocatalysis of CO tolerance in hydrogen oxidation reaction in PEM fuel cells. Electrochim Acta 1999;44:3283—93.
[8] Crabb EM, Marshall R, Thompesett. Carbon monoxide electro-oxidation properties of carbon-supported PtSn catalysts prepared using surface organometallic chemistry. J Electrochem Soc 2000;147:4440—7.
[9] Wang X, Hsing I-M. Kinetics investigation of H_2/CO electro-oxidation on carbon supported Pt and its alloys using impedance based models. J Electroanal Chem 2003;556:117—26.
[10] Arenz M, Stamenkovic V, Blizanac BB, Mayrhofer KJ, Markovic NM, Ross PN. Carbon-supported Pt—Sn electrocatalysts for the anodic oxidation of H_2, CO, and H_2/CO mixtures. Part II: the structure—activity relationship. J Catal 2005;232:402—10.
[11] García-Rodríguez S, Somodi F, Borbáth I, Margitfalvi JL, Peña MA, Fierro JLG, et al. Controlled synthesis of Pt-Sn/C fuel cell catalysts with exclusive Sn—Pt interaction application in CO and ethanol electrooxidation reactions. Appl Catal B 2009;91:83—91.
[12] Lim D-H, Choi D-H, Lee W-D, Lee H-I. A new synthesis of a highly dispersed and CO tolerant PtSn/C electrocatalyst for low-temperature fuel cell; its electrocatalytic activity and long-term durability. Appl Catal B 2009;89:484—93.
[13] Liu Z, Jackson GS, Eichhorn BW. PtSn intermetallic, core—shell, and alloy nanoparticles As CO-tolerant electrocatalysts for H_2 oxidation. Angew Chem Int Ed 2010;49:3173—6.
[14] Liu Y, Li D, Stamenkovic VR, Soled S, Henao JD, Sun S. Synthesis of Pt_3Sn Alloy nanoparticles and their catalysis for electro-oxidation of CO and methanol. ACS Catal 2011;1:1719—23.
[15] Herranz T, García S, Martínez-Huerta MV, Peña MA, Fierro JLG, Somodi F, et al. Electrooxidation of CO and methanol on well-characterized carbon supported PtxSn electrodes. Effect of crystal structure. Int J Hydrogen Energy 2012;37:7109—18.
[16] Michalak WD, Krier JM, Alayoglu S, Shin J-Y, An K, Komvopoulos K, et al. CO oxidation on PtSn nanoparticle catalysts occurs at the interface of Pt and Sn oxide domains formed under reaction conditions. J Catal 2014;312:17—25.

[17] Zhang Z, Ge J, Ma L, Liao J, Lu T, Xing W. Highly active carbon-supported PdSn catalysts for formic acid electrooxidation. Fuel Cells 2009;09:114–20.
[18] Cable RE, Schaak RE. Low-temperature solution synthesis of nanocrystalline binary intermetallic compounds using the polyol process. Chem Mat 2005;17:6835–41.
[19] Silva MR, Ângelo ACD. Synthesis and characterization of ordered intermetallic nanostructured PtSn/C and PtSb/C and evaluation as electrodes for alcohol oxidation. Electrocatal 2010;1:95–103.
[20] White PS, Rordgers JR, Page YL. CRYSTMET: a database of the structures and powder patterns of metals and intermetallics. Acta Cryst B 2002;B58:343–8.
[21] Innocente AF, Ângelo ACD. Electrocatalysis of oxidation of hydrogen on platinum ordered intermetallic phases: kinetic and mechanistic studies. J Power Sources 2006;162:151–9.
[22] Santos E, Pinto LMC, Soldano G, Innocente AF, Ângelo ACD, Schmickler W. Hydrogen oxidation on ordered intermetallic phases of platinum and tin – a combined experimental and theoretical study. Catal Today 2013;202:191–6.
[23] Pinto LMC, Juárez MF, Ângelo ACD, Schmickler W. Some properties of intermetallic compounds of Sn with noble metals relevant for hydrogen electrocatalysis. Electrochim Acta 2014;116:39–43.